Key technology of crop precision sowing based on the vision principle

Bing Li, Jiyun Li

College of Modern Information Technology, Henan Polytechnic, Zhengzhou, China

Abstract

The growth of crops is seriously affected in the process of precision planting of crops due to many external environmental interference factors, low precision of sowing technology, and large significant relative errors. To solve this problem, machine vision technology is introduced to study the key technology of crop precision sowing based on the vision principle. After pre-processing the crop image, the corresponding histogram is established. Then, the segmentation threshold method is used to gray the image and determine the best threshold to have a good recognition effect. Finally, according to the growth height and colour analysis of crops in the image, predict the growth of crops and realise the precision sowing of crops. The comparative experimental results show that under the application of the new sowing technology, the estimation accuracy of the crop planting area is high, the recognition accuracy of planting position is also high, and the fertilisation uniformity is close to the actual data, which can provide an important basis for improving the quality of crop sowing.

significant relative errors. To solve this problem, machine vision technology is introduced to study the key technology of crop precision sowing based on the vision principle. After pre-processing the crop image, the corresponding histogram is established. Then, the segmentation threshold method is used to gray the image and determine the best threshold to have a good recognition effect. Finally, according to the growth height and colour analysis of crops in the image, predict the growth of crops and realise the precision sowing of crops. The comparative experimental results show that under the application of the new sowing technology, the estimation accuracy of the crop planting area is high, the recognition accuracy of planting position is also high, and the fertilisation uniformity is close to the actual data, which can provide an important basis for improving the quality of crop sowing.

Introduction

Agriculture is the source of life for a country and the economic lifeline of a country or region (Goodwin *et al*., 2022). With the vigorous development of the modern economy, agriculture's influence is also increasing daily. In the field of agricultural production, sowing for all kinds of crops is an essential operation. The quality and accuracy of sowing directly impact the growth and production of subsequent crops. At present, some modern technologies have been applied to agricultural production, and precision sowing technology has become an important component in crop sowing (Virk *et al*., 2020). However, the problem of uneven yield caused by uneven fertilisation in agricultural planting areas has gradually emerged.

Booth *et al*. (2020) proposed the first robot vision framework to estimate the growth direction of plant bulbs. The framework takes three X-ray images as input and extracts shape, edge, and texture features from each image. Then these features are input into the machine learning regression algorithm to predict the two-dimensional projection of the bulb growth direction. This method provides an important reference for sowing by predicting the growth direction of the corn. Ni (2021) proposed a precision seeder navigation technology method based on the joint positioning of optics and ultrasound. Through the methods of ultrasonic ranging and laser scanning, the positioning of the operation area of the seeder and the planning of the walking path are realised, and the seeder's adaptability and autonomous operation level are improved. This method provides mechanised support for the precision seeder technology, but there are problems, such as low accuracy of the extraction of the sowing area. Oad *et al*. (2020) used remote sensing technology to identify the changes in rice sowing and harvest dates. During the study, geo-referenced crop samples, farmers' perception survey data, Landsat images, and climate data in the Lacana region were used. According to the results, remote sensing technology can obtain high-quality sowing images, which provides a reference for this technology.

Talaat *et al*. (2020) proposed an advanced automation system for electric vehicle charging based on machine vision and the

finite element method. This method uses machine vision and Internet of things technology to design an intelligent control system so electric vehicles can obtain the optimal value of WPT. Machine vision has a high level of automation, reliability, and inheritance in practical applications. Therefore, it is of great significance and influence to improve the accuracy of sowing technology. On this basis, aiming at the problems of low precision and poor efficiency of sowing technology in the current crop sowing process, machine vision technology is introduced to optimise the design of the key technology of precise sowing of crops.

Materials and Methods

Image acquisition structure model

The overall structure model of crop precision sowing image acquisition is shown in Figure 1. In order to develop the automatic acquisition and recognition of crop precision sowing image based on machine vision technology, the following steps shall be performed: i) the visual information acquisition model of crop precision sowing is constructed; ii) the infrared sensing information fusion tracking and recognition method is adopted (Fca and Phh, 2020); iii) the sensor information tracking node model of data sampling is constructed; and iv) the peripheral component interconnect extensions for instrumentation bus trigger method are adopted. Finally, the external clock bus of crop precision sowing image acquisition is obtained.

The matched filter detection model of crop precision sowing image is constructed, and h is set as the pixel set of crop precision sowing remote sensing image, assuming 3×3. The sub-block template matching detection method adopts the scale subdivision method to construct the crop precision sowing image and the empirical wavelet analysis method (Yi and Liu, 2021). Within the empirical scale range defined in the frequency domain, the information feature detection output of the crop precision sowing image is (θ^e, ρ^e). through the local quantitative feature decomposition method; the fuzzy block feature matching model for tracking the sensing information of crop precision sowing image is expressed as follows:

$$\left. \begin{array}{l} X = \{x \mid x \in [0, h]\} \\ Y = \rho^e \cos \theta^e \\ Z = \rho^e \sin \theta^e \end{array} \right\} \tag{1}$$

where x represents the sensing and tracking information of crop precision sowing images. The three-dimensional feature distribution structure of crop precision sowing image is used to realise information reorganisation. The three-dimensional information sub-band analysis model of crop precision sowing image fusion is constructed using fuzzy information fusion and feature clustering methods. The three-dimensional information fusion tracking control model $W(x)$ of crop precision sowing image is constructed by using the method of fuzziness detection (Fue *et al.*, 2021). The ambiguity detection characteristic component is obtained as follows:

$$ftiness(x) = \begin{cases} W(x), & if\ feasible \\ 1 + rW(x), & otherwise \end{cases} \tag{2}$$

Image blur operation is roughly divided into three steps. The first step is to set a reference value X_T (usually taken as the maximum grey level I_{max} in the image) and use a function T_1 (called fuzzy membership function) to map the grey level n_{ij} corresponding to the pixels (i, j) in the image n to the fuzzy field relative to the reference value:

$$\mu_{ij} = T_1(n_{ij}) \tag{3}$$

In this way, an $M \times N$-ary image x with L grey levels is mapped into a fuzzy set U, and each element in the set is a fuzzy membership degree relative to X_T, that is:

$$U = \bigcup_{j=1}^{N} \bigcup_{i=1}^{M} \frac{\mu_{ij}}{n_{ij}} \tag{4}$$

In the second step, a crossover point is selected, and the fuzzy membership degree is nonlinear transformed with the membership degree μ_c corresponding to the crossover point μ_c as the boundary:

$$\mu_{ij} = E_r(\mu_{ij}) \tag{5}$$

where o represents the number of image acquisition times.
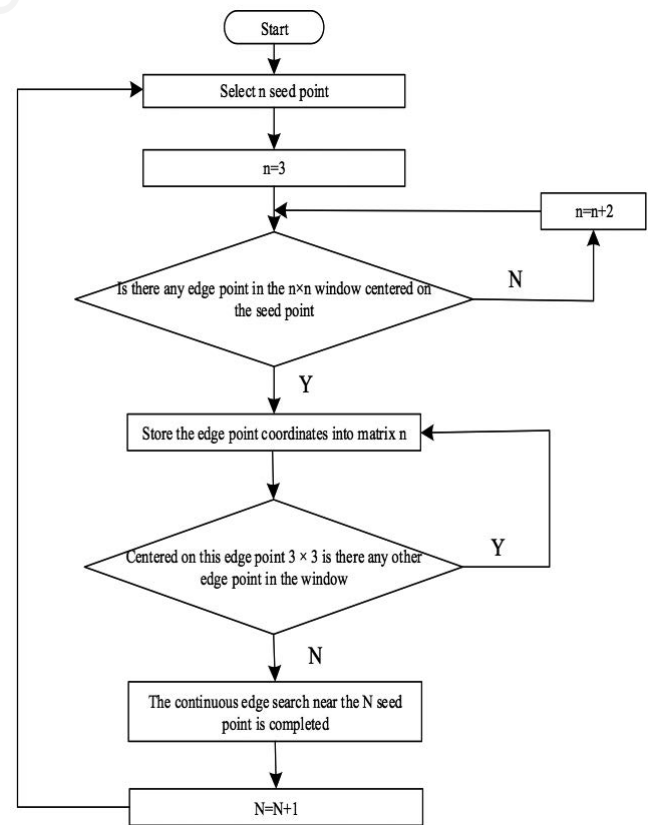
Figure 1. Image acquisition model of crop precision sowing.

The third step is to carry out fuzzy inverse mapping and map the obtained fuzzy membership to the image domain:

$$n_{ij} = T_2(\mu'_{ij}) \tag{6}$$

where $T_2(.)$ is often taken as the inverse transformation of $T_1(.)$ in equation (1). The final output result is:

$$X' = [n'_{ij}]_{M \times N} \tag{7}$$

where r is the central fusion degree. Build the edge retention model of crop precision sowing image, analyse the correlation information detection model of multiple high-frequency sub-band crop precision sowing images through statistical information analysis method, take ρ^e-R as the pixel clustering centre of crop precision sowing image, and analyse the key information feature points z of crop precision sowing image based on sparse feature expression method. The edge scale of high-frequency fusion of crop precision sowing image is obtained by using the method of central pixel fusion:

$$Team(z) = ftiness(x) - \arg(z + \rho^e - R) \tag{8}$$

In the method of low-frequency component fusion, the regular feature quantity of crop precision sowing image is obtained. The method of threshold matching is established, and the detail fusion model of crop precision sowing source image is constructed. The extraction results of crop precision sowing texture features are as follows:

$$sim(x, \rho^e - R) = \sum_{z=1} x \times Team(z) \tag{9}$$

In block area, $M \times N$, get the sub-block feature distribution set of the texture feature distribution of the crop precision sowing image, extract the edge contour feature of the crop precision sowing image under the machine vision, and improve the optimal acquisition and information extraction ability of the crop precision sowing image.

Crop sowing image pre-processing

In order to realise the research on the key technology of crop precision sowing, it is necessary to pre-process the obtained crop sowing image. In the crop sowing area, in the application of machine vision technology, the initialisation stage of visual navigation is unknown, so it is impossible to distinguish the images between crops and soil, and compared with other images, the crop sowing images have more obvious diversity and inconsistency (Akhter *et al.*, 2020; Zhao *et al.*, 2022). Given this characteristic, it is necessary to segment the image and process the grey image level when extracting the region and detecting the subsequent accuracy.

In the crop sowing area, observe the crop sowing through machine vision navigation, which is basically green, while the colour of the soil and surrounding environment is non-green. Therefore, based on this feature, in the crop sowing image, the original three-dimensional colour image is transformed into a one-dimensional grey image based on the feature of 2grb colour. Through the above operation and processing, it can reduce the data processing volume of later precision detection and further high-

light the information of crops. After grey processing, the grey image histogram of crops is shown in Figure 2.

As shown in Figure 2, there are obvious peaks in the image, but the valleys are not evident, and the corresponding areas are difficult to judge intuitively. At the same time, the grey value of the crop sowing area is usually large, while the grey value of other areas is small (Yang *et al.*, 2021; Zheng *et al.*, 2021).

After the greyscale processing of the crop sowing image is completed, it is segmented on this basis. Based on the basic idea of sub-region independent segmentation, this paper uses the combination of dynamic threshold and region segmentation to segment the relatively complex crop sowing image. The Otsu algorithm is used to select the threshold of the image area to be detected (Li *et al.*, 2017; Zhang *et al.*, 2021). In order to improve the accuracy of subsequent detection, noise reduction is also required for this area. Then, combination 3×3, extract the machine vision navigation line and corresponding discrete points and set the crop sowing image size to M×N. In this way, the pre-processing of crop-sowing image is completed according to the above contents, which provides a basis for subsequent target area extraction and accuracy detection (Tian *et al.*, 2021).

Extraction of planting area

Based on the above image pre-processing, the crop planting area is extracted.

Spectral angle matching

Through the spectral angle matching method, the time series curve corresponding to the pixel in the crop index time series data set is calculated (Gao *et al.*, 2020), and then the included angle value θ_i between the two curves is obtained:

$$\theta_i = \cos[X_i \cdot Y / |X_i| \cdot |Y|] \tag{10}$$

where X_i represents the time series curve corresponding to the i-th pixel, and Y represents the reference curve compared with it.

According to the above analysis, the above formula is transformed into the following formula:

$$\theta = \arccos \sum_{j=1}^{n} x_{ij} y_i / \sqrt{\sum_{j=1}^{n} x_{ij}^2 y_j^2} \tag{11}$$
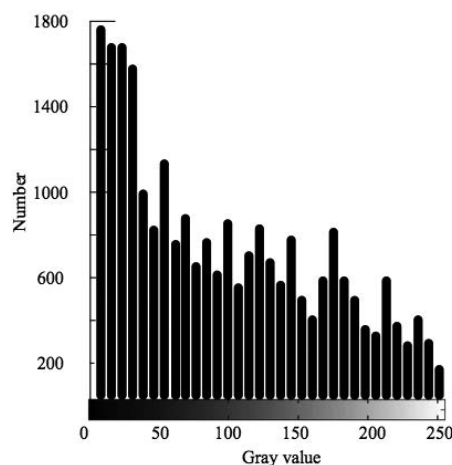
Figure 2. Histogram of grey image of crop sowing.

where x_{ij} represents the j-th vector point in the sequence curve composed of the i-th pixel, y_j represents the j-th vector point in the reference curve, and n represents the number of time nodes.

Threshold selection

According to the spectral angle value obtained from the above calculation, the rule remote sensing image threshold can be obtained (Abdollahzadeh *et al.*, 2021). The crop index time series curve corresponding to a sample is used as a vector, and the included angle radian between the sample and the time series curve is obtained through the following formula (12), that is, the included angle between θ_k line X_k and Y of the crop index time curve of sample point k:

$$\theta_k = \arccos(X_k \cdot Y)/|X_k| \cdot |Y| \tag{12}$$

Calculate the included angle corresponding to the sample point, and then calculate the average value δ of all included angles and the standard deviation σ of all included angles:

$$\delta = \sum_{k=1}^{m} \theta_k / m \tag{13}$$

$$\sigma = \sqrt{\frac{1}{m} \sum_{k=1}^{m} (\theta_k - \delta)^2} \tag{14}$$

where m represents the number of sample points, and the sum of the average value δ of the included angle and the standard deviation σ of the included angle is the threshold ε, which is calculated as follows:

$$\varepsilon = \sigma + \delta \tag{15}$$

Extraction of planting area

Based on the above-calculated threshold data, the average value and standard deviation of the angle between the time series curve and the sample are obtained, which are δ_{NEVI} and σ_{NDVI}, respectively. Furthermore, the average value and standard deviation of the angle between the time series reference curve and the sample point of the whole planting area can also be obtained, which are δ_{EVI} and σ_{EVI}, respectively.

$$\begin{cases} \delta_{NEVI} = 0.146 \\ \sigma_{NDVI} = 0.051 \\ \delta_{EVI} = 0.171 \\ \sigma_{EVI} = 0.064 \end{cases} \tag{16}$$

The threshold ε corresponding to the crop area in the study area is calculated through the standard deviation σ and the average value δ. The threshold δ_{NDVI} and ε_{EVI} of the rule image are obtained based on the NDVI time series data set and EBI time series set. The calculation formulas are as follows:

$$\begin{cases} \varepsilon_{NDVI} = \delta_{NDVI} + \sigma_{NDVI} \\ \varepsilon_{EVI} = \delta_{EVI} + \sigma_{EVI} \end{cases} \tag{17}$$

Compare the threshold value ε with the spectral angle value θi. If the spectral angle value θi is less than the threshold value ε, set the target figure in the i-th pixel. Then, the target pixel is extracted by using the rule image obtained by the threshold ε_{NDVI} based on the NDVI time series data set (Towers and Poblete-Echeverría, 2021). Using the rule image obtained by threshold ε_{EVI} combined with EVI time series data set, the target pixel is extracted, and the extraction results of fertilisation area in the planting area are obtained through these two groups of data.

Monitoring of fertilisation uniformity in precision sowing area

The main process of monitoring fertilisation uniformity in precision sowing areas is as follows: i) Panchromatic data and multispectral fusion are carried out based on obtaining remote sensing images of planting areas (Addesso *et al.*, 2020); ii) For the fused remote sensing image, the first principal component monochrome map I is extracted by principal component analysis; iii) The watershed method is introduced into the process of fertiliser uniformity monitoring (Alfarisy *et al.*, 2020), the first principal component monochrome map I is segmented and processed, and the superpixel object is extracted; iv) the feature group of the monitoring area is constructed, including contour feature similarity, brightness feature similarity, and texture feature similarity; v) through the characteristic group, fertilisation uniformity monitoring is completed based on the random forest principle.

The monitoring process of fertilisation uniformity monitoring method in precision sowing area is shown in Figure 3.
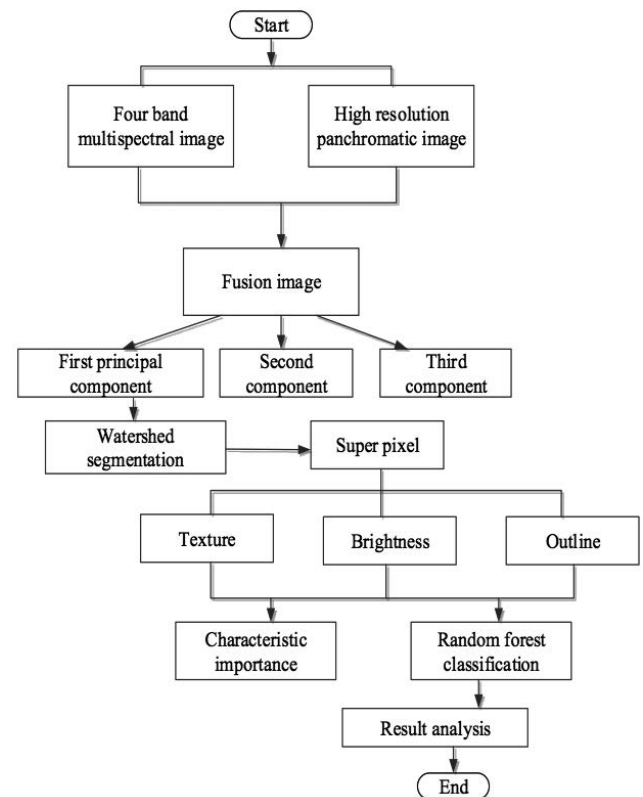
Figure 3. Flow chart of fertiliser uniformity monitoring.

Image segmentation

The concept of *superpixel* is introduced into the image processing of crop precision sowing. The superpixel image is obtained by the watershed segmentation algorithm.

In order to approximate the segmentation degree and verify the consistency between super-pixel and manual segmentation results, the monitoring method of fertilisation uniformity in precision sowing area adopts the method based on contour measurement (Yu *et al.*, 2021). Set the segmentation parameters. When the threshold T is 3, the segmentation effect of the remote-sensing image is the best. When k increases (k indicates the number of superpixels), the data to be processed also increases, which affects the efficiency of remote sensing image segmentation. In fertilisation uniformity monitoring, the precision sowing area fertilisation uniformity monitoring method sets the number of superpixels k to 1273, which can effectively complete the segmentation of remote sensing image of the planting area.

Feature set construction

Texture similarity

Calculate the χ^2-distance (also known as chi-square distance) between the histogram of super-pixel area, and the formula is as follows:

$$T(q,s) = \lg \frac{P_{same}[d_T(q,s)]}{P_{diff}[d_T(q,s)]} \tag{18}$$

where $T(q,s)$ represents the texture similarity of the two superpixel regions, q represents all superpixel objects as a whole, s represents the area of manual segmentation, $d_T(q,s)$ represents the χ^2 distance between the area of manual segmentation result s and the texture histogram of the superpixel object q, P_{same} represents the existence of superpixels in the manual segmentation region, and P_{diff} represents the existence of superpixels outside the manual segmentation region.

The sum of texture similarity of all super-pixel objects in the artificially segmented planting and fertilisation area is $T_1=\sum T(q,s)$; The sum of texture similarity of all super-pixel objects outside the artificially segmented planting and fertilisation area is $T_2=\sum T(q,s)$.

If the distance between several superpixels and the segmentation target is very close, the average value of their similarity can be taken.

Brightness similarity

The brightness description operator can reflect the histogram corresponding to the brightness values of different regions. Then, calculate the χ^2 distance between the histograms of each region, and normalise its logarithm.

The sum of the brightness similarity of all superpixel objects in the artificially segmented planting and fertilisation area is B_1; The sum of the brightness similarity of all super-pixel objects outside the artificially segmented planting and fertilisation area is B_2.

Contour energy

In order to reduce the adverse effect of the gradient region of the shadow image on the region boundary, the directional energy method is decided to detect the complex boundary more accurately. The formula for calculating directional energy is as follows:

$$OE_\theta = (I \times f_{1,\theta})^2 + (I \times f_{2,\theta})^2 \tag{19}$$

OE_θ represents the direction of energy in each pixel. When the value of direction angle θ is 0, the maximum value of direction energy is OE_0. by rotating f_1 and f_2 (where f_1 is the derivative of f Gaussian function and f_2 is the edge contrast calculated by f_1 based on filtering), if the value of all pixels adjacent to OE_θ under one direction scale is less than or equal to OE_θ, the direction energy is the maximum value. If the value of all pixels adjacent to OE_θ is greater than OE_θ in one direction scale, the maximum value is OE_θ.

Set the possibility value P_{con} through a nonlinear transformation in the interval [0,1]:

$$P_{con} = 1 - exp(-\frac{OE_\theta}{\sigma}) \tag{20}$$

where in order to reduce the noise caused by σ affecting the definition of remote sensing image, this paper decides to take the value of σ as 0.04 according to the data such as noise type, intensity, and remote sensing image target.

All superpixels are not in the divided area, but P_{con} and E_2 are on the edge, and all superpixels are P_{con} and E_1 in the divided area.

Monitoring of fertilization uniformity in the planting area

The monitoring method of fertilisation uniformity in precision sowing area is realised by the random forest method (Guo *et al.*, 2021).

The booting method, also known as the bagging method, is the main central idea of random forest classification. The general steps are as follows: extract several different samples from the original data set, randomly classify them according to the sample characteristics, and construct a complete classification tree. The detailed process is as follows: i) a super-pixel sample is randomly placed back while taking a super-pixel sample. k represents the total number of super-pixel samples. Assuming 500 times of extraction, N=500. Repeat this step to get a set of *ntree* super-pixel samples.

Because the accuracy will increase with the increase of the number of generated sample sets, however, the relevant processing data will also increase. Therefore, to balance the relationship between the two, *ntree* is selected as 100 according to the remote sensing image data, that is, *ntree* = 100. ii) Build a decision tree using the six feature attributes T_1, T_2, B_1, B_2, E_1, and E_2 constructed above, continue to construct the classification tree; iii) all sample sets repeat the first two steps to form a randomly classified forest; iv) if there are other remaining samples, their characteristics are determined by voting. When using the bagging method (Buthelezi *et al.*, 2020) to extract several sample sets with differences in the most original data set, it is required to quantitatively extract 63% of the most original sample set each time, and the extracted samples are called out of the bag (OOB).

In order to ensure the effectiveness of the above random forest classification method, it is decided to randomly extract a feature, record it as *f*, and test it. The calculation formula is as follows:

$$F^{(t)}(f) = \frac{\sum_{i=1}^{n} N(l_i = c_i^{(t)})}{|B|} - \frac{\sum_{i=1}^{n} N(l_i = c_{i,f}^{(t)})}{|B|} \tag{21}$$

where t represents the decision tree, B represents the data set of OOB, $c_i^{(t)}$ and $c_{i,f}^{(t)}$ represents the determination of x_i category of samples before and after feature f is removed, and N represents the counting function.

The uniformity measure of precision sowing area can be obtained from the average value of the importance of all decision trees:

$$F(f) = \frac{\sum_{}^{Ntree} F^{(t)}(f)}{Ntree} \tag{22}$$

According to the uniformity measurement of precision sowing area, we can know the growth trend of the existing planting process, which is the key technology to realising precision sowing of crops. After crop image pre-processing, the corresponding histogram is established according to the pre-processed image. By analysing the difference between the crop area and the growth background, the image is greyed by using the segmentation threshold method to determine the best threshold in the image so that the image has a good recognition effect. Finally, according to the growth height and growth colour analysis of the crop in the image, the growth trend of the crop is judged to realise the analysis and prediction of crop growth and provide a reference basis for the realisation of accurate planting of crops (Xie *et al.*, 2022).

Comparative experiment

Based on the introduction of machine vision technology, the above discussion proposed a precision sowing technology for crop sowing. In order to verify the effect of this method in practical application, the above sowing technology and the sowing technology of intelligent agricultural precision monitoring system are used in the same experimental environment, and their application effects are compared. Delphi7 is used to develop the system, and AVICap class in Delphi7 is used to create a video capture window in overlay mode to complete the call of the upper computer to the camera software development kit, which can effectively realize the real-time continuous transmission and display of video and image data after each sowing of the seed metering device. The image

acquisition results of the crop planting area are shown in Figure 4. In order to facilitate the discussion, the sowing technology based on machine vision is set as the experimental group, and the sowing technology of an intelligent agricultural precision monitoring system is set as the control group.

Experimental setup

The experimental environment comprises a driver, crop seeding box, seed box, capacitive sensor, bench, stepping motor, and other structures. The stepping motor with model 86BYGH250D and the driver with model HB-860H are used in the experiment, as shown in Figure 5. The seeder model is a petrol engine, and the six-row seeder is shown in Figure 6. The capacitive sensor with model CR18 is shown in Figure 7. The speed of seed metering wheel is adjusted by stepping motor, to control the flow of crops. The capacitance sensor device is used to collect the capacitance, and all the obtained data information is uploaded to the host computer to complete the comparison and analysis of the application effect of sowing technology. The control group method and the experimental group were used to record and count the data obtained from the experiment. Excel 2022 software was used to store and sort the collected data, and spss22.0 software was used to analyse the data. The software provides users with data mining, analysis, and decision-making solutions. Through SPSS 22.0 software, users can directly analyse various data in the database and filter out some abnormal problems with data samples and test data.

Figure 4. Image acquisition results of crop planting area.

Figure 5. 86BYGH250D stepper motor and HB-860H driver.

Results and Discussion

The seeds sown in the experiment are corn seeds. Firstly, the precision of seed sowing in single seed mode is detected, and the number of crops sown at the theoretical level is obtained. Then, the actual number of crop seeds in the receiving box is counted manually to obtain the actual number of crops. Finally, the detection accuracy of the two groups of sowing techniques is obtained by calculating the number of theoretical and actual crops. According to the above experimental contents, the comparative experiment on the detection effect of single seed sowing is completed, and the relevant experimental data are recorded, as shown in Table 1.

It can be seen from the data recorded in Table 1 that the number of sown grains of crops detected by the sowing technology of the experimental group is exactly the same as the actual number of grains, so there is no relative error; There is an error of 10-30 grains between the number of sown grains of crops detected by the sowing technology of the control group and the actual number of grains, so the relative error is in the range of 1.24-3.14%. In practical application, the relative error produced by the sowing technology of the control group will seriously affect the quality of crop sowing, failing to achieve the expected planting effect. In contrast,

the sowing technology of the experimental group can provide a more favourable data basis for crop sowing and ensure the planting effect.

Estimating planting area is an important index to monitor the uniformity of fertilisation in the planting area. Therefore, two methods are used to estimate the planting area respectively, and the estimation results are shown in Figure 8.

Figure 8 shows the estimated planting area of different methods. According to Figure 8, the estimated planting area of the precision planting area in the experimental group is close to the actual planting area, while the estimated planting area of the control group is quite different from the actual planting area. Compared with the test results of the above methods, the data close to the actual planting area can be obtained through the experimental group, which shows that the estimation effect of the experimental group is good because before the experimental group estimates the
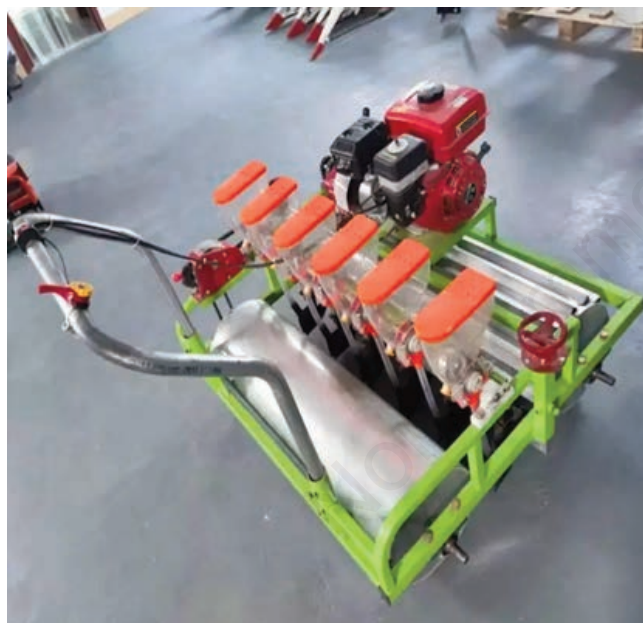
Figure 6. Petrol engine 6-Row seeder.

Figure 7. CR18 capacitance sensor.

Table 1. Comparison of drop accuracy of a single seed.

Number of experimental groups	Actual number of grains/piece	Test the number of grains in the experimental group/piece	The number of granules in the control group was detected/piece	Relative error of experimental group/%	Relative error of control group/%
1	803	803	785	0	2.24
2	912	912	892	0	2.19
3	911	911	889	0	2.41
4	924	924	895	0	3.14
5	806	806	796	0	1.24

planting area, the pixels of the planting area are obtained by using the spectral angle matching method. On this basis, the planting area is estimated, and the accuracy consistent with the actual area is improved.

Position recognition accuracy is to calculate the percentage of correct planting position in the whole planting area.

$$K = \sum_{j=1}^{n} \left| p_j - p_{j0} \right| \tag{23}$$

where K represents the position recognition accuracy of precision sowing area, P_j represents the percentage of the j-th planting area in the whole planting area measured by random forest method, P_{j0} represents the proportion of the j-th planting area in the large database area, and n represents the number of all planting areas involved in the experiment.

By analysing the data in Figure 9, it can be seen that with the increase of precise seeding area, the recognition rate of the seeding position of the experimental group and the control group continues to decline. However, under the same precise seeding area, the recognition rate of the experimental group is between 90 and 95%, and the recognition rate of the control group is between 85 and

90%. Therefore, the recognition rate of the experimental group is higher than that of the control group. Table 2 shows the uniformity measurement results of the above methods. According to the data in Table 2, the fertilisation uniformity data obtained by the experimental group is closer to the actual data than that of the control group, and the accuracy is higher than that of the control group.

The planting area of crops has the characteristics of broken plots, wide planted varieties, and high spatial distribution mixed degree. In order to precisely optimise the sowing efficiency of crops, this paper proposes a key technology for precision sowing of crops based on the principle of vision. In order to verify the application effect of this technology, a complete comparative experiment was designed. The experimental results proved that the number of seeds in the experimental group was exactly the same as the actual number of seeds, and the sowing accuracy was ideal. The error of the seeding technique in the control group was about 1.24-3.14%, and the application effect was worse. The estimated planting area of the technology studied in this paper completely accords with the actual planting area, indicating that this technology has better practical application performance. The planting location accuracy of the research technology can reach about 95%, and the average sowing uniformity is 93.03%, which has obvious advantages compared to traditional technology. Image pre-pro-

Table 2. Uniformity measurement results of fertilisation in planting areas with different methods.

Number of experiments/time	Uniformity/%		
	Expected value	Experience group	Control group
1	91.61	91.58	85.62
2	92.55	92.55	86.16
3	93.25	93.25	85.96
4	92.56	92.56	86.68
5	91.59	91.59	87.89
6	94.63	94.63	85.53
7	93.65	93.65	86.64
8	94.44	94.44	84.59
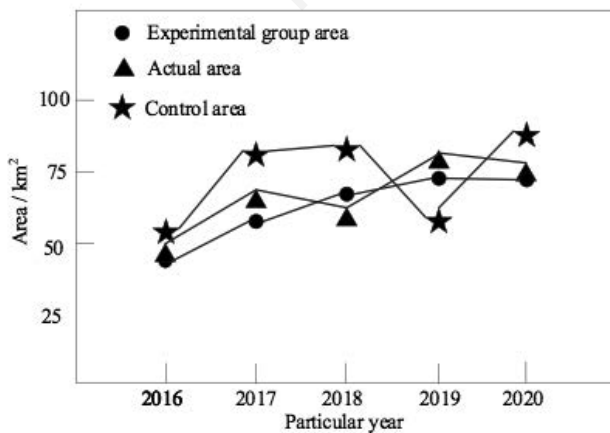
Figure 8. Estimation results of planting area by different methods.
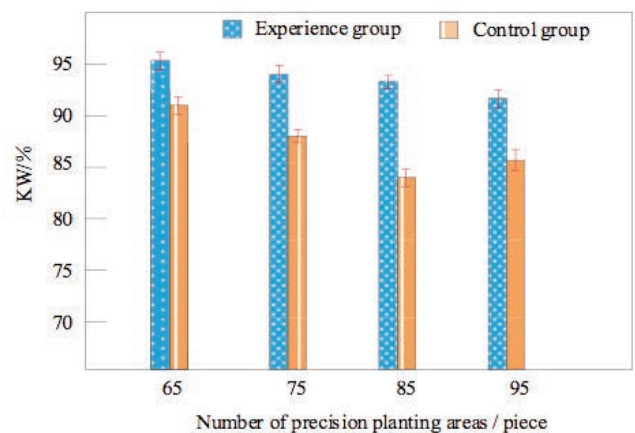
Figure 9. Comparison of planting position accuracy of different methods.

cessing is to check out each image to the recognition module recognition, which is called image pre-processing. The input image is processed in image analysis before feature extraction, segmentation, and matching. In this paper, crop seeding image pre-processing, crop seeding target area extraction, planting area extraction, and precision seeding area fertilisation uniformity monitoring to achieve precision sowing of crops, achieved better seeding effect, image pre-processing is the basis to ensure high-precision seeding.

Conclusions

The uniformity of fertilisation in the planting area determines the production efficiency, scientific and technological development, economic development, and living standard quality of various enterprises in a country, and also reflects the effectiveness of precision planting. Based on the above discussion and the introduction of machine vision technology, a new method of crop precision sowing process is proposed, and comparative experiments verify the application effect of this method. The key technology of precision seeding is proposed. Firstly, the crop area in the planting area is extracted to obtain the remote sensing image of the planting area. Then the image is classified to complete the remote sensing monitoring of the precision seeding area, which improves the reference for monitoring of the precision planting effect and lays a foundation for the informatisation of yield in the planting area and the improvement of agricultural production efficiency.

References

Abdollahzadeh S., Sepehr A., Rashki A. 2021. Detecting degraded, prone and transition ecosystems by environmental thresholds and spectral functions. Remote. Sens. Appl. Soc. Environ. 22: 100503.

Addesso P., Vivone G., Restaino R., Chanussot J. 2020. A data-driven model-based regression applied to panchromatic sharpening. IEEE. Trans. Image. Process. 29:7779-94.

Akhter M.J., Kudsk P., Mathiassen S.K., Bo M. 2020. Rattail fescue (Vulpia myuros) interference and seed production as affected by sowing time and crop density in winter wheat. Weed. Sci. 69:1-35.

Alfarisy F.K., Andriyani I., Bowo C. 2020. Evaluation of water quality due to the use of intensive fertilizer on farmer level in the upstream of bedadung jember watershed, East Java, Indonesia. J. Degraded. Min. Lands. Manage. 7:2301-12.

Booth B.G., Sijbers J., Beenhouwer J.D. 2020. A machine learning approach to growth direction finding for automated planting of bulbous plants. Sci. Rep. 10:661.

Buthelezi D., Mafeo T.P., Mathaba N. 2020. Preharvest bagging as an alternative technique for enhancing fruit quality: a review. Horttechnology. 31:1-10.

Fca B., Phh C. 2020. Prediction of human odour assessments based on hedonic tone method using instrument measurements and multi-sensor data fusion integrated neural networks. Biosyst. Eng. 200:272-83.

Fue K., Porter W.M., Barnes E., Rains G. 2021. Ensemble method of deep learning, color segmentation, and image transformation to track, localize, and count cotton bolls using a moving camera in real-time. Trans. ASABE. 64:341-52.

Gao X.Y., Li J., Zhang C.X. 2020. Similarity calculation of 3D model by integrating improved ACO into HNN. IEEE. Access. 8:155378-88.

Goodwin D., Holman I., Pardthaisong L., Visessri S., Ekkawatpanit C., Rey Vicario D. 2022. What is the evidence linking financial assistance for drought-affected agriculture and resilience in tropical Asia? A systematic review. Reg. Environ. Change. 22:1-13.

Guo B., Zhang D., Pei L., Su Y., Wang X., Bian Y., Zhang D., Wanqiang Y., Zhou Z., Guo L., 2021. Estimating PM2.5 concentrations via random forest method using satellite, auxiliary, and ground-level station dataset at multiple temporal scales across China in 2017. Sci. Total. Environ. 778:146288.

Li J., Xu K., Chaudhuri S., Yumer E., Zhang H., Guibas L. 2017. GRASS: generative recursive autoencoders for shape structures. ACM. T. Graphic. 36:1-14.

Ni J.N. 2021. Research on navigation technology of precision seeder based on optical and ultrasound joint positioning. J. Agric. Mec. Res. 43:211-15.

Oad V.K., Dong X., Arfan M., Kumar V., Mohsin M.S., Saad S., Lü H., Azam M.I., Tayyab M. 2020. Identification of shift in sowing and harvesting dates of rice crop (l. oryza sativa) through remote sensing techniques: a case study of larkana district. Sustainability. 12:1-15.

Talaat M., Arafa I., Metwally H., 2020. Advanced automation system for charging electric vehicles based on machine vision and finite element method. IET. Electr. Power. Appl. 14:2616-23.

Tian H., Qin Y., Niu Z., Wang L., Ge S. 2021. Summer maize mapping by compositing time series sentinel-1A imagery based on crop growth cycles. J. Indian. Soc. Remote. Sens. 49:2863-74.

Towers P.C., Poblete-Echeverría C. 2021. Effect of the illumination angle on NDVI data composed of mixed surface values obtained over vertical-shoot-positioned vineyards. Remote. Sens. 13:855.

Virk S.S., Fulton J.P., Porter W.M., Pate G.L. 2020. Row-crop planter performance to support variable-rate seeding of maize. Precis. Agric. 21:603-19.

Xie Y., Sheng Y., Qiu M., Gui F. 2022. An adaptive decoding biased random key genetic algorithm for cloud workflow scheduling. Eng. Appl. Artif. Intell. 112:104879.

Yang Y., Li T., Wang Y., Cheng H., Chang S., Liang C., An S. 2021. Negative effects of multiple global change factors on soil microbial diversity. Soil. Boil. Biochem. 156:108229.

Yi X.Q., Liu J. 2021. Wavelet threshold extraction method of local shadow feature of CT image. Comput. Simul. 38:181-4+403.

Yu H., Chen X., Ren M., Yin L., Wu Q., Zhan J., Liu Q. 2021. A coupled bend-twist deformation monitoring method based on inclination measurement and rational cubic spline fitting. Mech. Syst. Signal. Process. 147:107084.

Zhang X., Lu H., Guo D., Bao L., Huang F., Xu Q., Qu X. 2021. A guaranteed convergence analysis for the projected fast iterative soft-thresholding algorithm in parallel MRI. Med. Image. Anal. 69:101987.

Zhao Z.Y., Wang P.Y, Xiong X.B., Wang Y.B., Zhou R., Tao H.Y., Grace U.A., Wang N., Xiong, Y.C. 2022. Environmental risk of multi-year polythene film mulching and its green solution in arid irrigation region. J. Hazard. Mater. 435:128981.

Zheng W., Yin L., Chen X., Ma Z., Liu S., Yang B. 2021. Knowledge base graph embedding module design for Visual question answering model. Pattern. Recognit. 120:s108153.